Radiation Protection Dosimetry (2013), Vol. 154, No. 3, pp. 331–339 doi:10.1093/rpd/ncs235
Advance Access publication 5 September 2012

A STANDARD FOR ABSORBED DOSE RATE TO WATER IN A ^{60}CO FIELD USING A GRAPHITE CALORIMETER AT THE NATIONAL METROLOGY INSTITUTE OF JAPAN

Y. Morishita*, M. Kato, N. Takata, T. Kurosawa, T. Tanaka and N. Saito
National Metrology Institute of Japan, AIST, Tsukuba, Ibaraki 305-8568, Japan

*Corresponding author: aist-morishita@aist.go.jp

Received March 9 2012, revised July 30 2012, accepted August 4 2012

A primary standard for the absorbed dose rate to water in a ^{60}Co radiation field has been newly established at the National Metrology Institute of Japan. This primary standard combines the calorimetric measurements using a graphite calorimeter with the ionometric measurements using a thick-walled graphite cavity ionisation chamber. The calorimeter is operated in the constant temperature mode using AC Wheatstone bridges. The absorbed dose rate to water was determined to be 12 mGy s^{-1} at a point of 1 m from the radiation source and at a water depth of 5 g cm^{-2}. The uncertainty on the calibration coefficient in terms of the absorbed dose to water of an ionisation chamber using this standard was estimated to be 0.39 % ($k=1$).

INTRODUCTION

The absorbed dose to water is a quantity used in cancer radiotherapy. Many national metrology laboratories have established their own primary or secondary standards and they provide a direct calibration service to secondary laboratories or hospitals. This situation has been different in Japan. The National Metrology Institute of Japan (NMIJ) has established a primary standard for air kerma in a ^{60}Co field and calibrates ionisation chambers from secondary calibration laboratories. The secondary laboratories then determine their ^{60}Co field using the ionisation chamber and calibrate ionisation chambers from hospitals. In the hospital, the ionisation chamber is irradiated in a water phantom with high-energy X rays from a clinical linac and then the absorbed dose to water is determined by two conversions: one from the calibration coefficient in terms of air kerma to that of the absorbed dose to water in the ^{60}Co gamma rays and the other from the calibration coefficient in terms of the absorbed dose to water in the ^{60}Co gamma rays to that in the high-energy X rays, k_Q[1, 2]. However, the uncertainty of the former conversion is large at a value of around 1.3 %[2]. This results in a final dose uncertainty of ~2.3 % for high-energy X rays at the hospitals[3]. Although this uncertainty is within the acceptable level of 2.5 %[4, 5], it is desirable to further reduce the uncertainty in dose determination[6].

In response to this situation in Japan, the NMIJ has developed a standard for the absorbed dose rate to water in a ^{60}Co gamma-ray field and has started to offer the calibration service to the secondary laboratories. In this paper, the details of the primary standard, corrections to measurement results and uncertainty evaluations are reported.

^{60}CO RADIATION FIELD

A gamma-ray radiation field from a ^{60}Co source in the NMIJ is used to establish the primary standard for the absorbed dose rate to water. The source was renewed on January 2009, and its activity was 148 TBq at that time. The source is inside a thick-walled irradiator, which has a cylindrical collimator (diameter: 8 cm and length: 15.5 cm). The collimator is positioned ~150 cm above the ground and is oriented horizontally. The field diameter is ~11 cm at 1 m from the source. A wall to block radiation is located very far from the source; hence, back scattering from the wall is expected to be very low.

The irradiator has two shutters. One is a slow shutter installed in the irradiator. It takes ~20 s to open or close, but it blocks most radiation from the source. The other shutter is a fast shutter installed just downstream of the collimator. It takes ~0.3 s to open or close. Since there is a small gap between the collimator and the fast shutter, a small amount of the radiation escapes from the irradiator even when this shutter is closed. However, the radiation leakage is confirmed to be negligible near the measurement positions described below. Consequently, the fast shutter is used to start or stop the irradiation. The fast shutter operation is programmed on a computer outside of the irradiation room.

Two positioning laser systems produce the horizontal and vertical lines and their crossing point.

They are used to determine the position and orientation of a graphite cavity ionisation chamber, a calorimeter, a water phantom and an ionisation chamber. One laser marker perpendicular to the field axis is focused at a point of 1 m from the source. The other laser marker is located downstream of the field and it shows the centre of the field.

The water phantom used in the current measurements is installed on an experimental stage that can be translated in the axial field direction by 1–5 m from the source and in the radial field direction by 75 cm.

The temperature of the irradiation room is controlled around 22 ± 0.5°C. The humidity and the pressure are not controlled, but measurements are performed in a humidity range of 20–80 %, in which the humidity correction varies slowly[7]. The temperature, pressure and humidity are continuously recorded on computers during measurements and the data are used to correct the current from the graphite cavity ionisation chamber or the ionisation chamber.

CALORIMETRIC MEASUREMENTS

Instruments

Figure 1a shows a cross-sectional view of the graphite calorimeter of the NMIJ. The calorimeter is a Domen-type calorimeter[8]; a disk (called the core) is enclosed by a jacket (middle layer) and a shield (outermost layer). These three components are separated from each other by 1-mm gaps. The core is 20 mm in diameter and 2 mm in thickness, the jacket is 26 mm in diameter and 8 mm in thickness, and the shield is 32 mm in diameter and 14 mm in thickness. The walls of the jacket and the shield are 2 mm in thickness and are made of high-purity graphite (density: 1.97 g cm^{-3}). The mass of the graphite in the core was measured to be 1.217829 g using a calibrated mass comparator (AT21, Mettler Toledo). Table 1 shows the masses of constituents of the core. The core is kept in position by tensions of lead wires of thermistors (described below), while the jacket and the shield are kept in position by styrene spacers.

Two different kinds of thermistors are used as heaters and temperature sensors. Four thermistors (PB9-43, Shibaura Denshi) with resistances of ~10 kΩ at ~22°C are implanted in each of the graphite parts as heaters. The thermistor bead is typically 0.43 mm in diameter and 1-mm long and is assumed to be composed of MnO_2 and SiO_2 with a mass ratio of 1:1. Dumet wires with a diameter of 0.07 mm are connected to the thermistor. The wires are coated with polyimid for insulation. The wires have a chemical composition of Ni, Fe and Cu with a mass ratio of 2:2:1. The masses of a bead and wires of a different sample were measured and applied to the thermistors used in the core. The thermistor masses are found to have a standard deviation of <5 %.

For temperature measurements, two thermistors (BR14KA202K, Nikkiso-YSI) are implanted in the core and one thermistor is implanted each in the jacket and the shield. The beads of these thermistors are typically 0.36 mm in diameter and 0.8-mm long. The bead mass was measured in a similar manner as that of the heater thermistor and the result is included in Table 1. Platinum wires that are 0.03 mm in diameter are connected to the bead and they are coated with polyimid for insulation. These thermistors are calibrated at 273.15, 313.15 and 343.15 K. Resistances at these temperatures are typically ~4820, 1135 and 470 Ω, respectively. Substituting these calibration results into the Steinhart–Hart formula[9] and determining coefficients in the formula show a resistance near the calorimeter-operating temperature (296 K) of ~2000 Ω and a gradient (dR/dT) of −70 Ω/K. The heat capacity of graphite is typically $\sim 8.5\ J \cdot K^{-1} \cdot mol^{-1}$. Hence, when the core is irradiated with a dose of 1 Gy, the thermistor resistance is expected to change by 0.1 Ω (corresponding to a temperature change of 1.4 mK). Epoxy glue (Bob Smith Industries) is used to implant the thermistors in the graphite components.

The calorimeter thus assembled is mounted on a PMMA phantom (see Figure 1b) with styrene spacers. The phantom is square in shape (150 mm × 150 mm) and is 100 mm in thickness in the axial field direction. The calorimeter and the phantom are installed in a vacuum chamber made of PMMA. The front window of the chamber is 5 mm in thickness. For the electrical shielding, the chamber is enclosed by an aluminum housing except for the front window. The chamber is evacuated using an oil-free pump to <0.01 Pa. A graphite plate is placed in front of the chamber to adjust the effective mass thickness from the surface to the core centre to be 5 g cm^{-2}.

To determine the resistance (temperature), a Wheatstone bridge was tested while keeping in mind that a dose of 1 Gy irradiation changes the resistance of a 2000 Ω thermistor by 0.1 Ω. Two sets of measurement devices were prepared: one for DC operation and the other for AC operation. A nanovoltmeter (33420A, Agilent) was used as a null detector when the bridge was operated by a DC power supply (R6161, Advantest). A digital lock-in amplifier (LI5340, NF) was used as a null detector when the bridge was operated using an AC power supply. AC power was supplied from the lock-in amplifier at 413 Hz. The effective operation voltage was 0.1 V in both cases. Lines (A) and (B) in Figure 2 show the responses of the null detectors when one of the resistors in the Wheatstone bridge was changed by 0.1 Ω

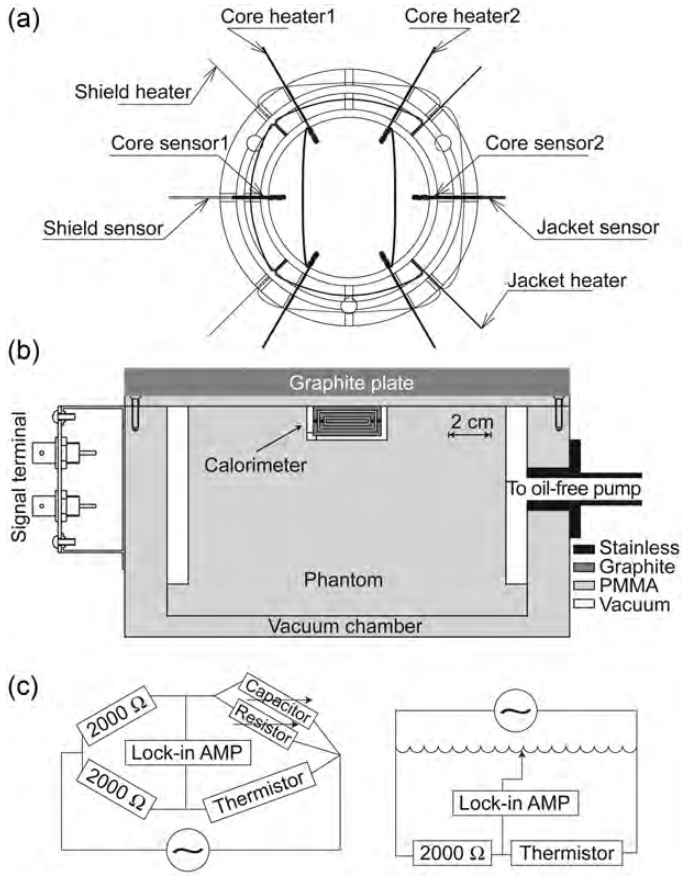

Figure 1. (**a**) A cross-sectional view of the graphite calorimeter; (**b**) the calorimeter mounted in PMMA phantom and (**c**) schematics of the Wheatstone bridge (left) and transformer bridge (right).

Table 1. Materials, masses and absorbed dose ratios of the core components.

Material	Mass (g)	D_i/D_G
Graphite disk		
C	1.217829	—
Wire		
Cu	0.0030096	1.331
Fe	0.0060192	1.238
Ni	0.0060192	1.349
Bead		
MnO_2	0.0010775	1.113
SiO_2	0.0010775	1.019
Epoxy		
$C_{18}H_{20}O_3$	0.0015740	1.084

from 2000 Ω in the DC and the AC bridges, respectively. The three remaining resistors were fixed at 2000 Ω. Both measurements exhibit similar responses, although background drift is observed in the DC operation. Despite trying hard to eliminate ground loops in the electrical circuit[10], the background of the DC measurement system cannot be stabilised. In contrast, it is easy to stabilise the background in AC operation; ground points are connected to earth as many as possible without considering the ground loop. The ratios between standard deviation of the background and the signal for the 0.1 Ω change are 1.2 and 0.3 % for DC and AC operation, respectively. AC operation is chosen for temperature measurements and two Wheatstone bridges and one transformer bridge are prepared. The transformer bridge (6415A and 1415C, SunJem) has a similar structure to the Wheatstone bridge. It also exhibits a similar response to the 0.1 Ω change, as shown by line (C) in Figure 2.

In calorimeter operation, the Wheatstone bridge is used for the shield and jacket and the transformer bridge is used for the core. The left side of Figure 1c shows a schematic of the Wheatstone bridge consisting of two 2000 Ω resistors, a thermistor and a

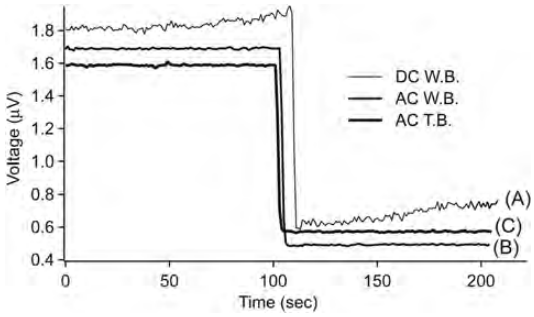

Figure 2. Responses of the null detectors when one of the resistors in the Wheatstone bridge is changed by 0.1 Ω from 2000 Ω for DC (line A) and AC (line B) operations. Line C shows the response in the transformer bridge.

variable resistor. A variable capacitor with a capacitance between 0 and 350 pF is connected in parallel to the variable resistor to adjust the phase at the lock-in amplifier. The right side of Figure 1c shows a schematic of the transformer bridge, in which a 2000 Ω resistor and a thermistor are connected in series. The voltage at the midpoint of these components is measured by the lock-in amplifier.

Measurements

The calorimeter is operated in the constant temperature mode[11]. The temperatures of the core, the jacket and the shield are controlled at a constant but different temperature by adjusting the currents to the heater thermistors. This is achieved by PID control programmed in LabView; each second, the program reads the outputs from the lock-in amplifiers through a GPIB bus, calculates the current outputs using the PID equation and then adjusts the outputs of the current sources connected to the heater thermistors. Three current sources (R6161, Advantest) are used. One of these sources is calibrated in terms of Ampere and used for the core heater. A calibrated voltmeter (2000, Keithley) is connected in parallel to the core heater. The target temperatures of the core, jacket and shield are ∼296.5, 296.2 and 295.9 K, respectively (the room temperature is ∼295.2 K).

The thin line in Figure 3a shows the output of the lock-in amplifier (left axis) for the core when the fast shutter of the ^{60}Co irradiator is repeatedly opened and closed once an hour. Here, the PID program controls the lock-in amplifier output to be zero. The lock-in amplifier output changes suddenly when the shutter is operated (shown by the arrows in the figure), but it returns to zero after several minutes due to the PID control. The thick line in Figure 3a shows the power (right axis) consumed by the heater thermistors of the core. Although the consumed power also changes suddenly when the shutter is operated, it exhibits a step-like behaviour. This difference in the consumed power corresponds to the power $P_{\mathrm{rad}}(c)$ supplied by the ^{60}Co field to the core. This measurement is performed 20 times. Figure 3b shows the resultant absorbed powers. The average power is ∼14.1 μW. The standard deviation of the data is ∼0.4 % (k=1) and the standard deviation of the mean is obtained to be ∼0.08 %.

The validity of these power measurements is confirmed as follows. As mentioned above, the core contains two temperature thermistors. When the calorimeter is operated, one temperature thermistor is used, while the other is not. Supplying known powers to this thermistor not being used repeatedly

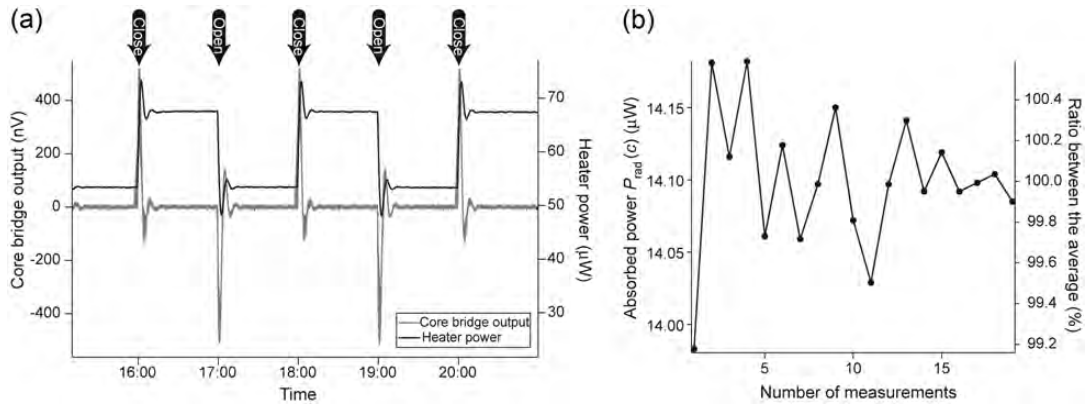

Figure 3. (**a**) The thin and thick lines indicate the lock-in amplifier output (left axis) and the heater power (right axis) of the core when the fast shutter is repeatedly opened and closed once an hour in the constant temperature mode. The steps observed in the heater power represent the powers absorbed by the core from the ^{60}Co field. (**b**) The resultant distribution of the absorbed powers.

like Figure 3a and comparing these supplied powers with the measured powers by the calorimeter, the validity can be confirmed. The comparison is performed by supplying a power of 7.8 μW to the thermistor. For 30 measurements, the measured data have a standard deviation of 0.8 % and a standard deviation of the mean of 0.14 %. The average measured power agrees with the supplied power within an accuracy of 0.05 %.

This measurement for validity also demonstrates that even though the power is supplied at a localised point in the core, the calorimeter response is correct.

ABSORBED DOSE RATE TO GRAPHITE

By correcting the power measured by the calorimeter $P_{\mathrm{rad}}(c)$, the absorbed dose rate to graphite $\dot{D}_{\mathrm{G}}(c)$ at a graphite depth of c=5 g cm^{-2} can be expressed as:

$$\dot{D}_{\mathrm{G}}(c) = \frac{P_{\mathrm{rad}}(c)}{M_{\mathrm{core}}} k_{\mathrm{gap}} k_{\mathrm{depth}}^{\mathrm{cal}} k_{\mathrm{imp}} k_{\mathrm{def}} k_{\mathrm{rad}} k_{\mathrm{axl}} \qquad (1)$$

The quantities in Equation (1) are as follows.

M_{core} is the mass of the core, which includes the graphite disk, the thermistors and the epoxy glue. The masses of these components were measured using the mass comparator. The results are tabulated in Table 1 in which the thermistor is divided into a lead wire and a bead.

The factor, k_{gap}, is the gap correction, which is defined as $k_{\mathrm{gap}} = D_{\mathrm{G}}^{\mathrm{fill}}(c')/D_{\mathrm{G}}^{\mathrm{gap}}(c)$, where $D_{\mathrm{G}}^{\mathrm{gap}}(c)$ is the expected absorbed dose by the calorimeter at a depth c and $D_{\mathrm{G}}^{\mathrm{fill}}(c')$ is the expected absorbed dose when all the gaps are filled with graphite; the depth in the latter case is greater than that in the former case because the gaps are filled with graphite. These two quantities are calculated using the Monte Carlo code, Electron Gamma Shower, version 5 (EGS5)[12]. The energy spectrum at 1 m from the ^{60}Co source has been calculated[13] using another Monte Carlo code (MCNP4[14]), in which scattered radiations by the irradiator, the collimator and a capsule of the source were taken into account. The resultant spectrum is used in the source routine and the EGS5 simulation is started from the front surface of the calorimeter. The angular distribution of photoelectrons, fluorescence after K- and L-photoelectric effects and Rayleigh scattering are taken into account using optional functions of the EGS5 code. The cut-off kinetic energy of photons and electrons is 10 keV. The uncertainty for k_{gap} is estimated by executing the code several times with different seeds for the random number generator. As a result, k_{gap}=0.9961 is obtained with an uncertainty of 0.1 %. In the following, unless otherwise noted, correction factors and their uncertainties are calculated in a similar manner.

Due to filling the gaps with graphite, the absorbed dose corrected by the gap correction corresponds to that at a point deeper than c. The factor, $k_{\mathrm{depth}}^{\mathrm{cal}}$, corrects this to the correct depth of c and is defined as $k_{\mathrm{depth}}^{\mathrm{cal}} = D_{\mathrm{G}}^{\mathrm{fill}}(c)/D_{\mathrm{G}}^{\mathrm{fill}}(c')$. By performing EGS5 simulations, $k_{\mathrm{depth}}^{\mathrm{cal}} = 1.0135$ is obtained with an uncertainty of 0.15 %.

The factor, k_{imp}, is called the impurity correction and it is defined as the ratio of the mass to the effective mass of the core[15];

$$k_{\mathrm{imp}} = \frac{M_{\mathrm{G}} + \sum_i M_i}{M_{\mathrm{G}} + \sum_i M_i (D_i/D_{\mathrm{G}})} \qquad (2)$$

Here, M is the mass and the subscripts G and i, respectively, indicate the graphite disk and impurities (thermistor and epoxy) in the core. D_{G} and D_{i} are the absorbed dose to the core disk and impurities. These are estimated by the products of the photon energy fluence and the mean mass energy-absorption coefficient $(\bar{\mu}_{en}/\rho)$. The photon energy fluence is evaluated at the centre of the core using the EGS5 code. The mean mass energy-absorption coefficient is calculated using those for the monoenergetic energy photons[16] and the photon energy spectrum. Table 1 lists the molecular formulae, the masses and the absorbed dose ratios used in the calculation. From these results, k_{imp}=0.9961 is obtained with an uncertainty of 0.05 %. This uncertainty results mainly from uncertainties in the physical constant.

The factor, k_{def}, is known as the heat defect; it is conventionally taken to be k_{def}=1.0000 for graphite.

The factors, k_{rad} and k_{axl}, are the radial and axial corrections. These corrections result from the fact that the quantity to be determined is at point c, but the core spreads in both the axial and radial directions and the absorbed dose also varies in these directions. The dose distribution in the axial direction of the core is simulated and k_{axl}=1.0003 is obtained as the ratio between the dose at the core centre and that averaged along the axial direction of the core. The dose distribution along the radial direction has been measured in the air kerma standard[13], from which k_{rad}=1.0000 is obtained.

Although the distance between the radiation source and the core centre and the depth of the core centre from the calorimeter surface do not appear in Equation (1), uncertainties arising from these quantities are considered. The laser marker used to measure 1 m from the source has a line width of 1 mm. The measured dose is expected to be proportional to the inverse of the distance squared, and the setting position of the calorimeter is

uniformly distributed around ± 0.5 mm. The uncertainty for the distance was then obtained as $2 \times 0.5/1000 \times 100/\sqrt{3} \approx 0.06\%$. The measured dose is expected to decrease according to $e^{-(\mu/\rho)_G x}$, where x is the core depth and $(\mu/\rho)_G$ is the mass attenuation coefficient of graphite. The calorimeter was fabricated with a precision of 0.1 mm and the graphite density is $\sim$1.9 g cm^{-3}. Hence, the uncertainty due to the depth is evaluated to be $\sim$0.06 % for 1.25-MeV photons.

Table 2a lists the quantities used to determine the absorbed dose rate to graphite and their uncertainties.

IONOMETRIC MEASUREMENTS

The absorbed dose rate is next converted from graphite to water. This is achieved by performing the measurements using a thick-walled graphite cavity ionisation chamber. Figures 4a and b show the cross-sectional views of the graphite cavity ionisation chamber. The cavity is enclosed by the high-purity graphite wall (indicated by the hatched regions in the figures). Most of the the other areas are made of PMMA or cable components. The graphite wall has an outer diameter of 32 mm and a thickness of 14 mm, which are the same dimensions as those of the calorimeter shield. The wall and the centre electrode are 4.85 and 0.3 mm in thicknesses, respectively. The total graphite and air thicknesses along the axial direction are 10 and 4 mm, respectively, which are also the same as those of the calorimeter.

An electric potential of $\pm$ 150 V is applied to the cavity wall. Charges collected by the centre electrode are accumulated in a standard capacitor with a capacitance of 1000 pF or 10 nF. The accumulated charge is measured by a calibrated vibrating-reed electrometer (TR8401, Takeda Riken). Typical currents measured at opposite electric potential polarities are within 0.01 % of each other and the mean value is taken as the measured current. The reference temperature, pressure and humidity are taken to be 0°C, 101.325 kPa and 0 %, respectively.

It is necessary to measure the currents for two cases to determine the conversion factor to convert the absorbed dose to graphite to that to water. In one case, the graphite cavity ionisation chamber is placed in a phantom similar to the calorimeter, whereas it is placed in a water phantom in the other case.

A PMMA phantom and chamber that have almost the same dimensions as the calorimeter are prepared. Placing the graphite cavity ionisation chamber in this phantom and adding the graphite plate used in the calorimetric measurement to adjust the depth, the centre of the electrode of the graphite cavity ionisation chamber, whose effective mass thick is 5 g cm^{-2}, is aligned at the 1 m position using the laser markers. The graphite cavity ionisation chamber is then irradiated and the current $k_{T'P'}k_{h'}I_G$ under the reference conditions is measured.

Next the graphite cavity ionisation chamber is encased in a PMMA waterproof sleeve with a wall thickness of 2 mm and it is inserted in a PMMA water phantom with dimensions of 350 mm (radial direction), 400 mm (axial direction) and 350 mm (height) and a wall thickness of 13 mm. A portion of the front side of the phantom has a thin window (thickness: 3 mm; diameter: 180 mm) to allow the incident radiation to enter. There are two linear stages on the top of the phantom that move independently of each other in the radial and axial directions. The axial stage has a digital scale that can determine its position with a precision of 0.01 mm. The radial stage has a holder that grips the cavity ionisation chamber. The phantom is filled with $\sim$45 L of distilled water. A calibrated thermocouple is placed in a waterproof cylinder and is positioned in the water at the same height as the chamber cavity.

Thin lines are drawn on both sides of the phantom at a water depth of 10 cm. The position of the graphite cavity ionisation chamber is adjusted so that these lines and the centre of the chamber are visually aligned. The reproducibility of determining the chamber position by this method is confirmed by performing several trials, which has a standard deviation of $\sim$0.15 mm. The chamber is moved in the axial direction by 5 cm (as measured by the digital scale) so that it is positioned at a depth of 5 cm in water. The experimental stage (on which the phantom sits) is translated so that the centre of the chamber is located at the laser marker from perpendicular to the field; the distance between the chamber and the radiation source is 1 m.

Since the density of water is $\sim$0.9978 g cm^{-3} at 22°C, the water depth of 5 cm is $\sim$0.2 % shallower than 5 g cm^{-2} in units of mass thickness. On the other hand, the thin window of the phantom expands due to the weight of the water, which increases the water depth. Figure 5 shows the displacement of the centre of the thin window when the phantom is filled with water. This displacement is measured using a laser displacement sensor. The sensor is first calibrated by displacing it by 1 mm [(a) in Figure 5]. As soon as filling commences (b), the measured point starts to slowly expand. When the water level reaches the bottom of the window (c), the measured point expands faster and it continues to do so until filling stops. The total displacement is $\sim$0.4 mm. Similar displacements are obtained when the phantom is filled with the same amount of water. Summarising the above, the water depth is

Table 2. Quantities and uncertainties for the standard for the absorbed dose rate to water.

Quantity	Unit	Value	A type (%)	B type (%)
(a) Quantities and uncertainties for the absorbed dose rate to graphite				
$P_{rad}(c)$	W	1.4260×10^{-5}	0.15	0.022
M_{core}	kg	1.2366×10^{-3}	0	0.0003
k_{gap}		0.9961	—	0.1
k_{depth}^{cal}		1.0135	—	0.15
k_{imp}		0.9961	—	0.05
k_{def}		1.0000	—	0.1
k_{axl}		1.0003	—	0.01
k_{rad}		1.0000	—	0.02
Distance and depth uncertainties		1.0000	—	0.08
$\dot{D}_G(c)$[a]	Gy s^{-1}	1.160×10^{-2}	0.15	0.23
(b) Quantities and uncertainties for the conversion from graphite to water				
$I_W k_{TP} k_h / I_G k_{T'P'} k_{h'}$		0.9677	0.09	—
k_{sl}		1.0009	—	0.1
k_{depth}^{cav}		1.0135	—	0.15
$(\bar{\mu}_{en}/\rho)_G^W$		1.1127	—	0.14
β_G^W		1.0003	—	0.05
Ψ_G^W		1.0103	—	0.15
Distance and depth uncertainties		1.0000	—	0.14
R_G^W		1.075	0.09	0.31
(c) Quantities and uncertainties for the calibration coefficient				
$\dot{D}_W(t)$[a]	Gy s^{-1}	1.246×10^{-2}	0.17	0.33
Decay correction		0.9440	—	0.036
I[b]	A	2.1733×10^{-10}	0.03	0.05
$k_{TP}k_h$		1.0000	—	0.04
Distance and depth uncertainties		1.0000	—	0.08
N	Gy C^{-1}	5.41×10^{7}	0.18	0.35

[a]1 May 2009.
[b]8 October 2009.

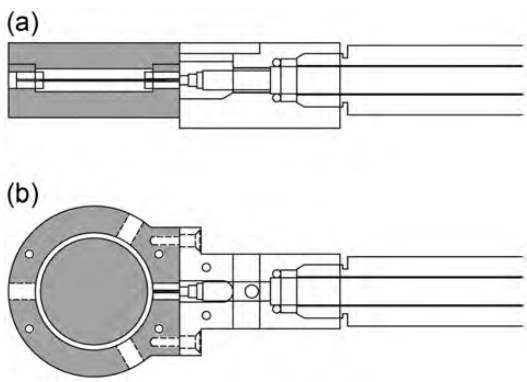

Figure 4. Cross-sectional views of a graphite cavity ionisation chamber: (**a**) side and (**b**) front views.

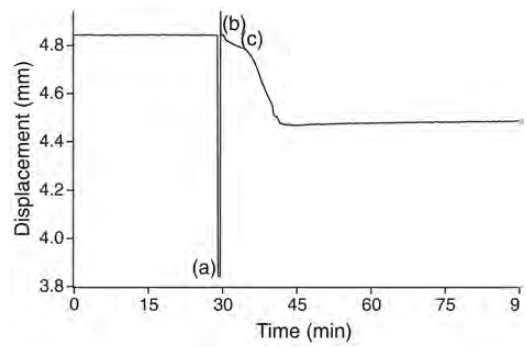

Figure 5. Displacement of the centre of the thin window of the water phantom. Calibration by 1-mm displacement is performed at (a), filling with water commences at (b) and the water level reaches the bottom of the thin window at (c). The total displacement due to filling is ~0.4 mm.

50.4 mm, which corresponds to a mass thickness of ~5.03 g cm^{-2}.

Irradiating the graphite cavity ionisation chamber thus installed in the water phantom, a current $k_{TP}k_hI_W$ is obtained under the reference conditions. The ratio of $k_{TP}k_hI_W$ to $k_{T'P'}k_{h'}I_G$ is 0.9677.

ABSORBED DOSE RATE TO WATER

Applying cavity theory to the measured currents in the calorimeter and water phantoms, the ratio of the absorbed dose rate to graphite to that to water can be written as

$$R_{\mathrm{G}}^{\mathrm{W}} = \frac{k_{\mathrm{TP}} k_{\mathrm{h}} I_{\mathrm{W}}}{k_{\mathrm{T'P'}} k_{\mathrm{h'}} I_{\mathrm{G}}} \frac{k_{\mathrm{sl}}}{k_{\mathrm{depth}}^{\mathrm{cav}}} \left(\frac{\bar{\mu}_{\mathrm{en}}}{\rho}\right)_{\mathrm{G}}^{\mathrm{W}} \beta_{\mathrm{G}}^{\mathrm{W}} \Psi_{\mathrm{G}}^{\mathrm{W}} \tag{3}$$

Here, the scheme in ref. (17) is applied to the current measurement in the water phantom; specifically, the air in the cavity is first replaced with graphite (hereafter, referred to as the intermediate state) to give the absorbed dose to graphite and the graphite is then replaced with water.

The factor, k_{sl}, in Equation (3) corrects the difference between the waterproof sleeve and the water. By performing similar simulations for the calorimeter corrections, $k_{\mathrm{sl}}=1.0009$ is obtained.

The factor, $k_{\mathrm{cav}}^{\mathrm{depth}}$, is similar to $k_{\mathrm{cal}}^{\mathrm{depth}}$ in Equation (1). Applying the cavity theory to the current measurement in the calorimeter phantom, air in the graphite cavity ionisation chamber is replaced with graphite, which makes the centre of the electrode in the cavity chamber deeper than 5 g cm^{-2}. This factor corrects the depth to 5 g cm^{-2}. Because the graphite cavity ionisation chamber is designed in such way that the air and graphite wall thicknesses are the same as the gap and graphite thicknesses in the calorimeter, it is expected that $k_{\mathrm{cav}}^{\mathrm{depth}} \approx k_{\mathrm{cal}}^{\mathrm{depth}}$. The gap in the calorimeter is vacuum, whereas the cavity is filled with air. However, the calculations in this study reveal that this produces a difference of only 0.03 %. Thus, $k_{\mathrm{cav}}^{\mathrm{depth}} = k_{\mathrm{cal}}^{\mathrm{depth}}$ is a good approximation. This means that the absorbed dose rate to water and its uncertainty are not affected by these factors.

In Equation (3), $(\bar{\mu}_{\mathrm{en}}/\rho)$ is the mean mass-energy absorption coefficient, β is the absorbed dose to kerma factor and Ψ is the energy fluence. The superscript W and the subscript G indicate that these quantities are evaluated at a water depth of 5 g cm^{-2} (W) and the centre of the graphite in the intermediate state (G), respectively. The ratio of these quantities gives $(\bar{\mu}_{\mathrm{en}}/\rho)_{\mathrm{G}}^{\mathrm{W}}$, $\beta_{\mathrm{G}}^{\mathrm{W}}$ or $\Psi_{\mathrm{G}}^{\mathrm{W}}$. By performing Monte Carlo calculations, $(\bar{\mu}_{\mathrm{en}}/\rho)_{\mathrm{G}}^{\mathrm{W}} = 1.1127$, $\beta_{\mathrm{G}}^{\mathrm{W}} = 1.0001$ and $\Psi_{\mathrm{G}}^{\mathrm{W}} = 1.0103$ are obtained.

Table 2b shows the parameters that make up the conversion factor $R_{\mathrm{G}}^{\mathrm{W}}$ and their uncertainties. Here, similar to the corrections for the calorimeter, the uncertainties arising from the 1 m distance from the source and depths in water and the calorimeter phantoms are considered. From $\dot{D}_{\mathrm{G}}(c)$ by the calorimeter and $R_{\mathrm{G}}^{\mathrm{W}}$ by the graphite cavity ionisation chamber, the absorbed dose rate to water at 5 g cm^{-2} in the water phantom is determined to be $\dot{D}_{\mathrm{G}}(c)R_{\mathrm{G}}^{\mathrm{W}}$; its value was $\sim$12 mGy s^{-1} in May 2009.

CALIBRATION

Calibration is usually performed with a farmer-type ionisation chamber. The chamber is set in the water phantom in the same way as the graphite cavity ionisation chamber and the current obtained by irradiating in the ^{60}Co field is measured. The absorbed dose rate to water as a function of time t is given by

$$\dot{D}_{\mathrm{W}}(t) = \dot{D}_{\mathrm{G}}(c) R_{\mathrm{G}}^{\mathrm{W}} \left(\frac{1}{2}\right)^{(t-t_0)/T} \tag{4}$$

where t_0 is the time when the absorbed dose rate to water is determined and T is the half-life of ^{60}Co (5.2417$\times$365.2422 d). By correcting the air conditions to the reference conditions (generally, 22°C, 101.325 kPa and 50 %), and dividing $\dot{D}_{\mathrm{W}}(t)$ by this, the calibration coefficient $N_{\mathrm{D,W}}$ is obtained as

$$N_{\mathrm{D,W}} = \frac{\dot{D}_{\mathrm{W}}(t)}{k_{\mathrm{TP}} k_{\mathrm{h}} I} \tag{5}$$

where $k_{\mathrm{TP}} k_{\mathrm{h}} I$ is the current from the ionisation chamber in the reference conditions. Table 2c shows the quantities that make up the calibration coefficients and their uncertainties for a PTW TN-30013 ionisation chamber. The uncertainty in the calibration coefficient is evaluated to be 0.39 % (k=1).

As stated above, the water depth in the water phantom is a little deeper than 5 g cm^{-2} because the thin window expands due to the weight of the water. The output currents at various water depths are measured for the ionisation chamber (PTW TN-30013) and the graphite cavity ionisation chamber. The water depth is changed from 5.0 to 4.5 cm, while the distance between the ^{60}Co source and the chambers is fixed at 1 m. The calibration coefficients vary randomly within $\pm$0.1 %; i.e. no systematic change is observed. This demonstrates that the calibration depth is not a critical factor for the calibration coefficient if the chambers are inserted in the water phantom with the same procedure.

SUMMARY

In summary, a national primary standard for the absorbed dose rate to water in a ^{60}Co gamma-ray field was established by combining a graphite calorimeter and a thick-walled graphite cavity ionisation chamber. The calorimeter is operated in the constant temperature mode with AC Wheatstone bridges, and the absorbed dose rate to graphite was determined.

The thick-walled graphite cavity ionisation chamber was used to determine the conversion factor from graphite to water and measurements were performed in water and calorimeter phantoms. Correction factors for the measured results were calculated by the EGS5 Monte Carlo code. The absorbed dose rate to water was determined to be $\sim$12 mGy s^{-1} at 1 m from the ^{60}Co source for an 11-cm radiation field and a water depth of 5 g cm^{-2} (May 2009). The uncertainty for the calibration coefficient of the ionisation chamber in terms of the absorbed dose to water with this standard was estimated to be 0.39 % (k=1).

The standard explained here has been compared with the Bureau International des Poids et Mesures (BIPM)[18] and the results showed that the calibration coefficients of the NMIJ were 0.4 % smaller than those of the BIPM. This difference was within the uncertainty calculated from uncertainties of both laboratories.

The calibration service will soon be started within the framework of the Japan Calibration Service System (JCSS) which is based on the ISO/IEC 17025, and the dose uncertainty of high-energy X rays at end users by the clinical linac is estimated to improve from 2.3 to 1.5 % (k=1)[3].

REFERENCES

1. IAEA. Absorbed Dose Determination in External Beam Radiotherapy. Technical Report Series No. 398. IAEA. (2000).
2. Japan Society of Medical Physics, Ed. *Standard dosimetry of absorbed dose in external beam radiotherapy (Standard Dosimetry 01)*. (2002) (in Japanese).
3. Sakata, S., Takase, N., Katayose, T., Yamashita, W., Yajima, K., Narita, K., Mizuno, H., Fukumura, A., Shinbo, M. and Jpn, J. J. Med. Phys **32**(Suppl. 1), no. 277. Private communication (2012) (in Japanese).
4. ICRU. *Determination of absorbed dose in a patient irradiated by beams of X or gamma rays in radiotherapy procedures*. ICRU Report No. 24. ICRU (1976).
5. AAPM. *Physical aspects of quality assurance in radiation therapy*. AAPM Report No. 13. American Institute of Physics (1994).
6. AAPM. *Tissue inhomogeneity corrections for megavoltage photon beams*. AAPM Report No. 85. American Institute of Physics (2004).
7. ICRU. *Average energy required to produce an ion pair*. ICRU Report No. 31. ICRU (1979).
8. Domen, S. R. and Lamperti, P. J. A. *A heat loss compensated calorimeter: theory, design and performance*. J. Res. NBS A **78**, 595 (1974).
9. Steinhart, I. S. and Hart, S. R. *Calibration curves for thermistors*. Deep Sea Res. **15**, 497 (1968).
10. Williams, A. J. and Rosser, K. E. *A comparison of A.C. and D.C. Wheatstone bridges for the purpose of high precision temperature measurement*. NPL Report CIRM42. National Physical Laboratory (2000).
11. Daures, J. and Ostrowsky, A. *New constant-temperature operating mode for graphite calorimeter at LNE-LNHB*. Phys. Med. Biol. **50**, 4035 (2005).
12. Hirayama, H., Namito, Y., Bielajew, A. F., Wilderman, S. J. and Nelson, W. R. *The EGS5 code system*. SLAC-R-730 (2005) and KEK Report 2005-8 (2005).
13. Kurosawa, T., Takata, N., Koyama, Y. and Kato, M. *AIST monograph of metrology,* No. 7. National Metrology Institute of Japan (2005) (in Japanese).
14. Briesmeister, J. F., Ed. *MCNP-A general Monte Carlo N-particle transport code, Version 4A*. LANL Report LA-12625. Los Alamos National Laboratory (1993).
15. DuSautoy. *The UK primary standard calorimeter for photon-beam absorbed dose measurement*. Phys. Med. Biol. **41**, 137 (1996).
16. Hubbell, J. H. and Seltzer, S. M. *Tables of X-ray mass attenuation coefficients and mass energy-absorption coefficients 1 keV to 20 MeV for elements Z = 1 to 92 and 48 additional substances of dosimetric interest.* NISTIR Report 5632. National Institute of Science and Technology.
17. Boutillon, M. and Perroche, A-M. *Ionometric determination of absorbed dose to water for cobalt-60 gamma rays*. Phys. Med. Biol. **38**, 439–454 (1993).
18. Kessler, C., Allisy-Roberts, P. J., Morishita, Y., Kato, M., Takata, N., Kurosawa, T., Tanaka, T. and Saito, N. *Comparison of the standards for absorbed dose to water of the NMIJ and the BIPM for ^{60}Co γ-ray beams*. Metrologia **48**, 06008 (2011).